Electronic Supplementary Material (ESI) for Molecular Systems Design & Engineering.
This journal is © The Royal Society of Chemistry 2017

Supplementary Information

2D and 3D-printing of self-healing gels: design and extrusion of self-rolling objects

*Milena Nadgorny, Zeyun Xiao and Luke A. Connal**

Department of Chemical and Biomolecular Engineering, the University of Melbourne, Parkville,

Victoria 3010, Australia

*E-mail: luke.connal@unimelb.edu.au

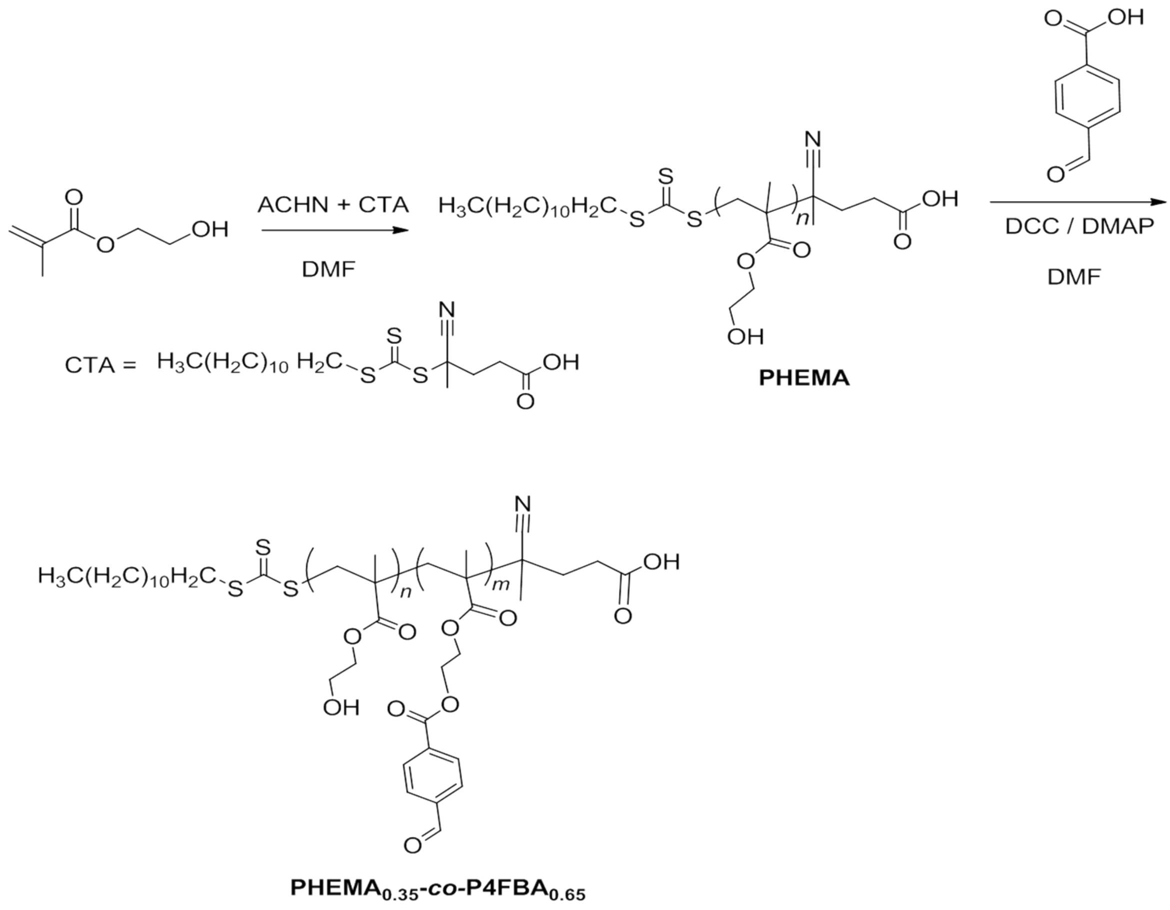

Scheme S1. Synthesis of benzaldehyde-functionalized PHEMA (PHEMA$_{0.35}$-*co*-P4FBA$_{0.65}$). PHEMA is synthesized by RAFT polymerization. Facile post-polymerization functionalization with 4-formylbenzoic acid (4FBA) by Steglich esterification results in benzaldehyde-functionalized PHEMA (n=0.35, m=0.65 for 1 equivalent of DCC and 4FBA).

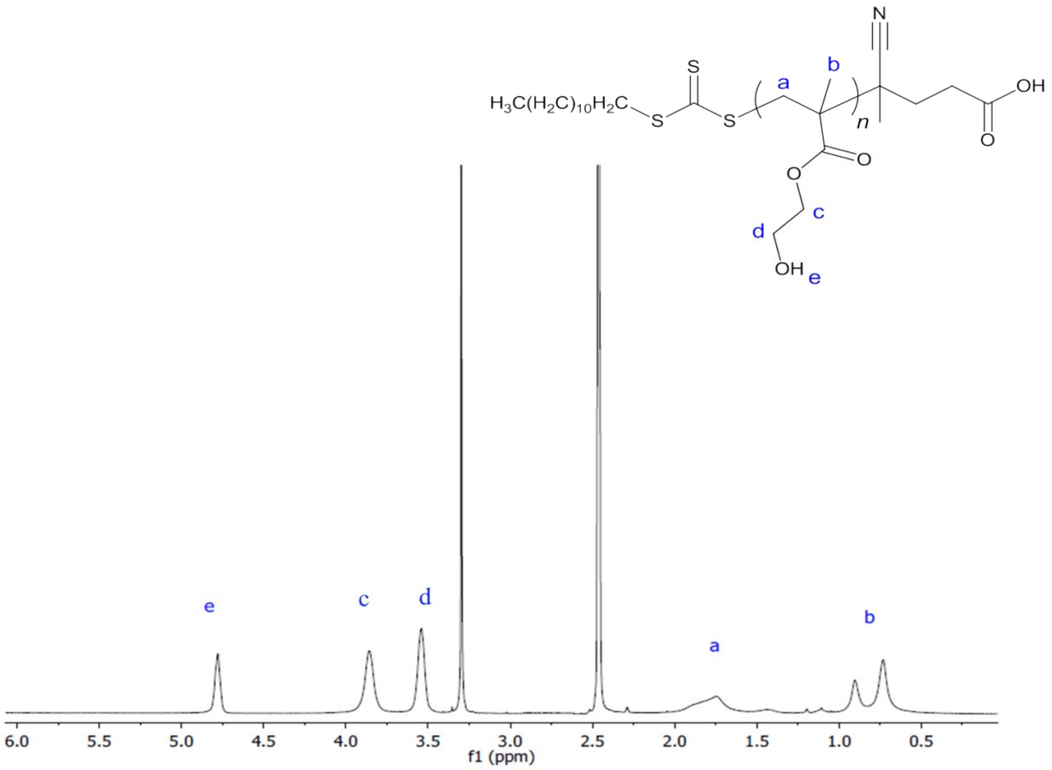

Figure S1. ^{1}H NMR spectrum of the synthesized PHEMA in DMSO-d_6. Chemical shifts: δ=4.78 ppm signal is attributed to the hydroxyl proton (e); δ=3.86 ppm corresponds to -OC$\mathbf{H_2}$C protons (c); δ=3.54 ppm represents –C$\mathbf{H_2}$OH protons (d); δ=1.74 ppm represents the protons of the aliphatic backbone of PHEMA (a); δ=0.90 ppm and δ=0.73 ppm correspond to the protons of the methyl group on PHEMA backbone (b).

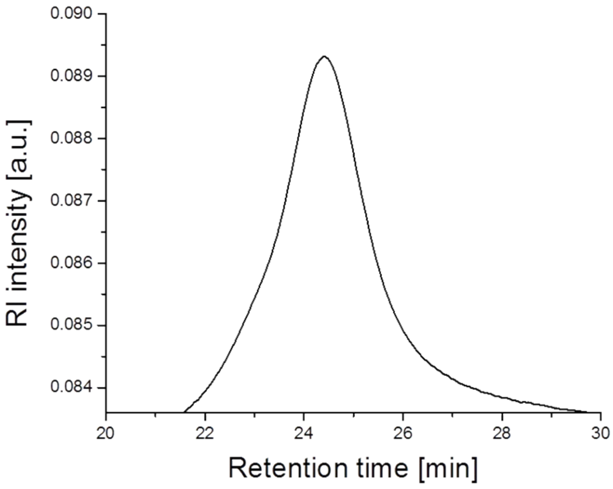

Figure S2. SEC traces of the synthesized PHEMA (M_n= 31 kDa, $Đ$ =1.36). Peak broadening and tailing can be attributed to the polymer interactions with the SEC column.[1]

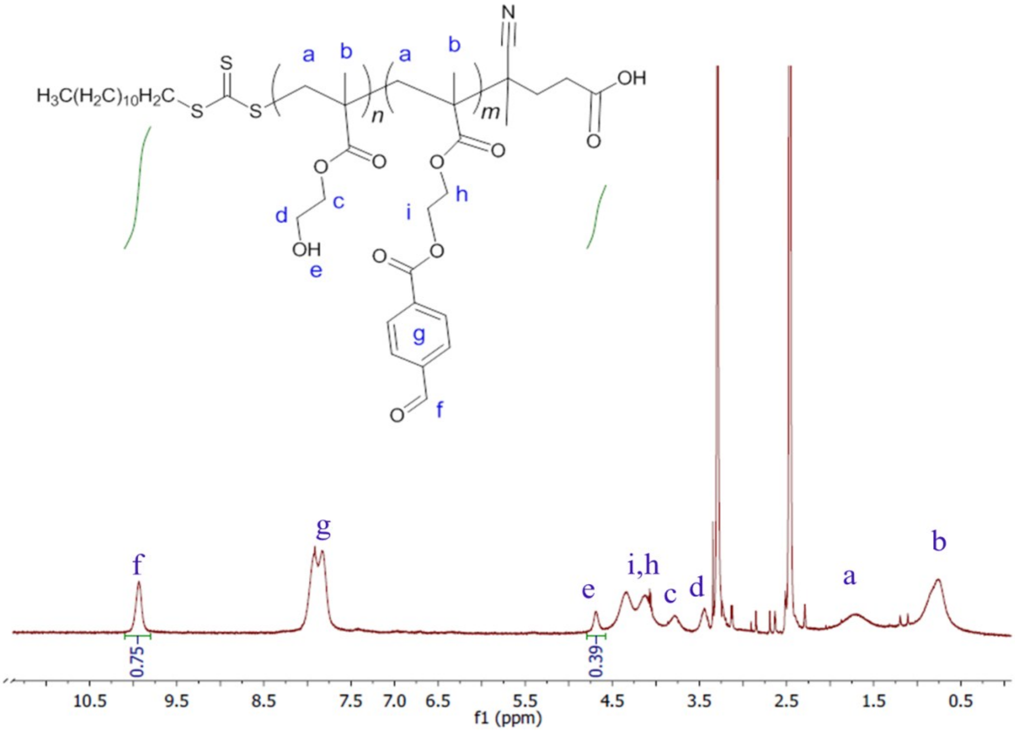

Figure S3. ^{1}H NMR spectrum of PHEMA functionalized with 4FBA (PHEMA$_{0.35}$-*co*-P4FBA$_{0.65}$) in DMSO-d_6. Chemical shifts: δ=9.93 ppm is attributed to the aldehyde proton (f); δ=7.88 ppm corresponds to aromatic protons of the benzene ring (g); δ=4.69 ppm is attributed to the protons of unfunctionalized hydroxyl groups (e); δ=3.78 ppm corresponds to–OC**H$_2$**C of unfunctionalized PHEMA units (c); δ=3.45 ppm is attributed to–C**H$_2$**OH of unfunctionalized PHEMA units (d); δ=4.32 ppm and δ=4.12 ppm are attributed to –OC**H$_2$**C protons of functionalized PHEMA units (h,i) ; δ=1.73 ppm represents the protons on the aliphatic backbone of the polymer (a); δ=0.76 ppm represents protons of the methyl group on the backbone of the polymer (b).

A successful esterification is supported by an appearance of a broad aldehyde peak at 9.93 ppm and an appearance of a broad aromatic peak at 7.88 ppm, which is attributed to the protons of the benzene ring of 4FBA. The conversion of alcohols to aldehydes was calculated by comparing the integration of the aldehyde signal (f) to the alcohol signal (e): *n*=0.35, *m*=0.65 for 1 eq. 4FBA.

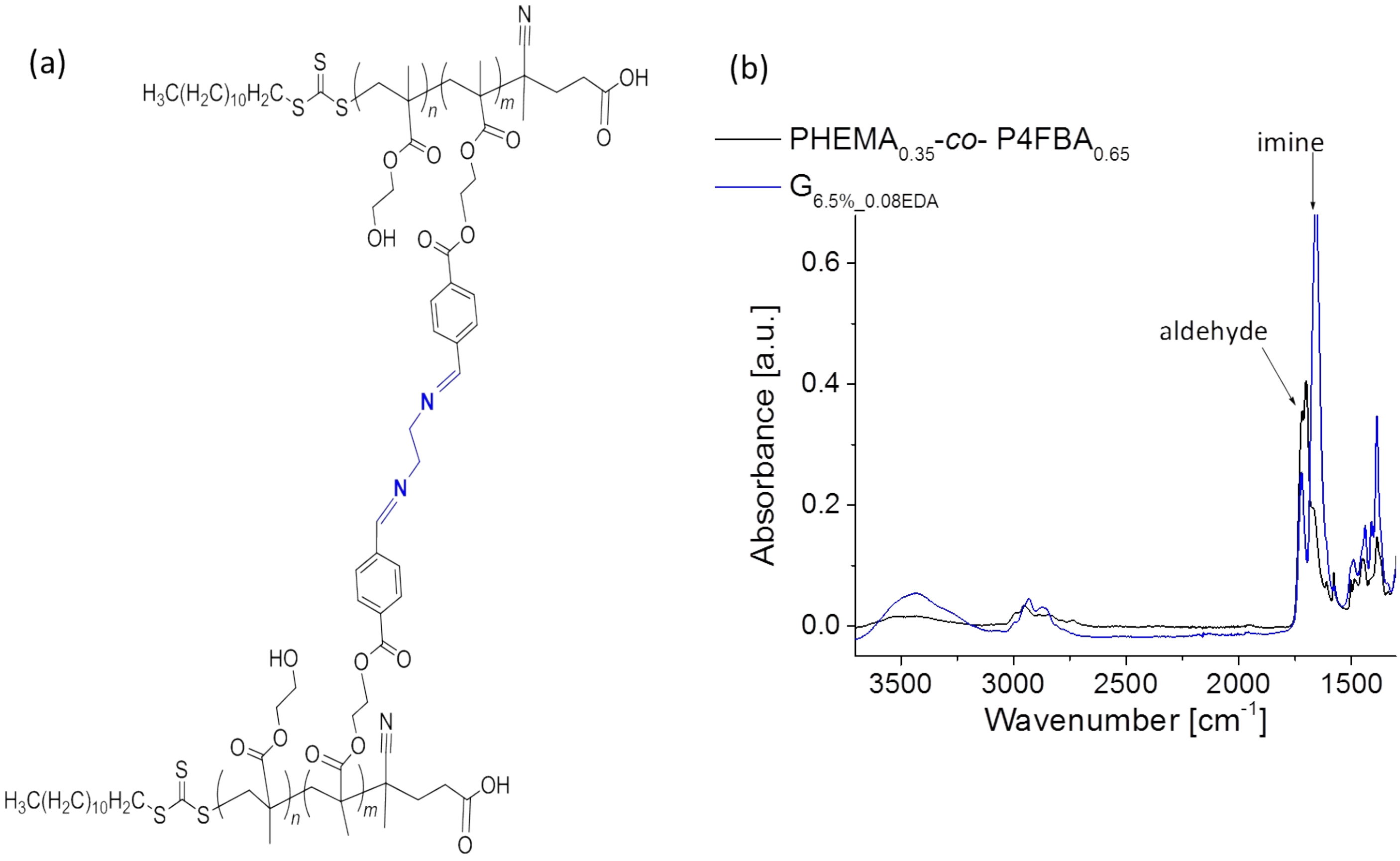

Figure S4.(a) Chemical structure of self-healing gels prepared from PHEMA$_{0.35}$-*co*-P4FBA$_{0.65}$ cross-linked with EDA. The reaction between aldehydes and amines allows a formation of dynamic imine bonds. (b) FTIR spectrum of G$_{6.5\%\_0.08EDA}$ demonstrates a decrease in the aldehyde signal at 1720 cm^{-1} and a formation of a new imine peak at 1660 cm^{-1}, indicating a successful cross-linking.

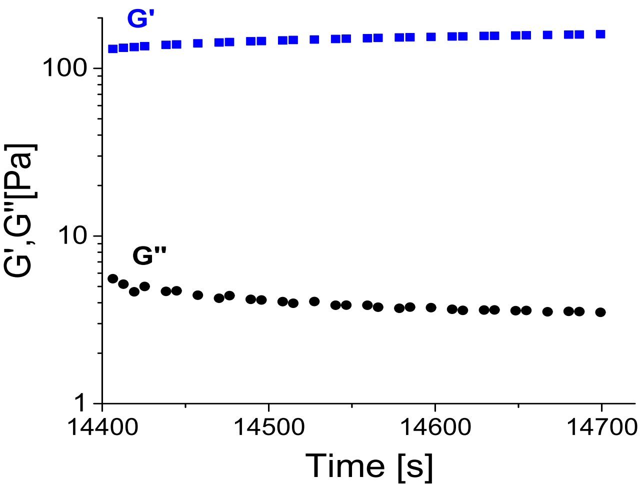

Figure S5. Dynamic moduli of $G_{6.5\%\_0.08EDA}$ 4 hours after preparation. G' plateau at ~150 Pa indicates that the moduli stabilize about ~5 min. post preparation and don't exhibit any significant further growth.

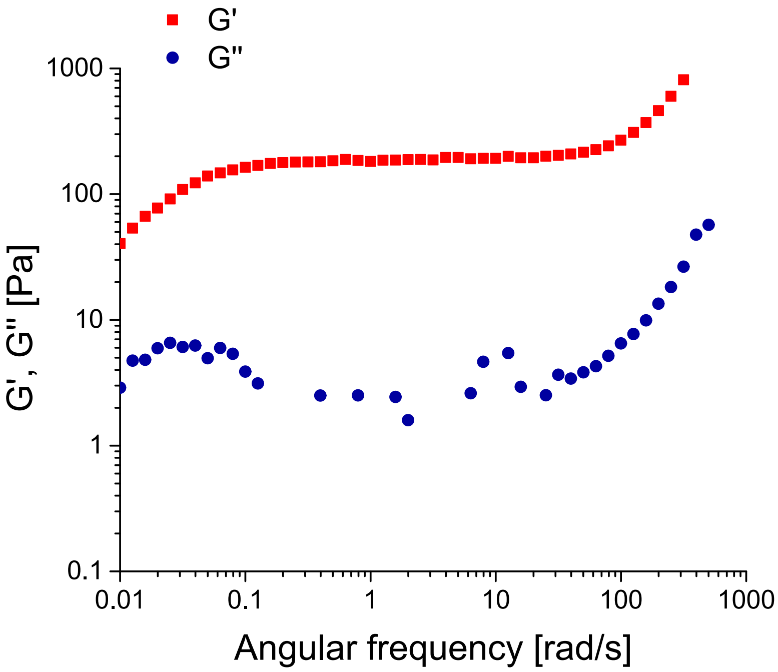

Figure S6. Frequency sweep shows that the moduli of $G_{6.5\%\_0.08EDA}$ are frequency dependant.

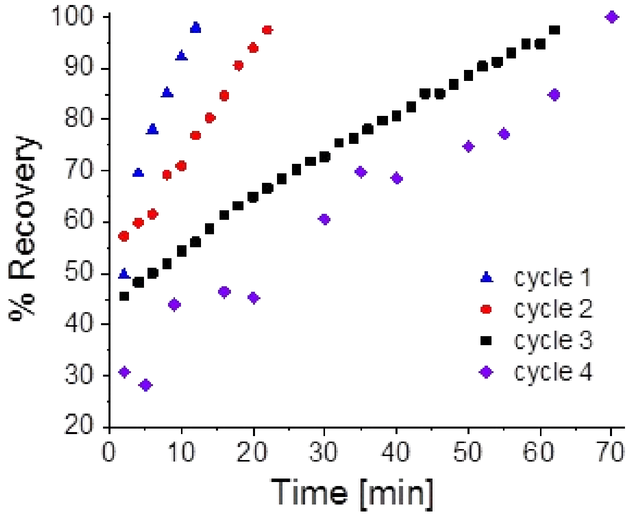

Figure S7. Recovery performances of $G_{6.5\%\_0.08EDA}$ from repetitively induced mechanical damages. The recovery time increases with the increasing number of breaking-healing cycles from 12 min to 22 min, 62 min and 70 min at the 1st, 2nd, 3rd and 4th cycle, respectively. For all the examined cycles, ~98% recovery was achieved.

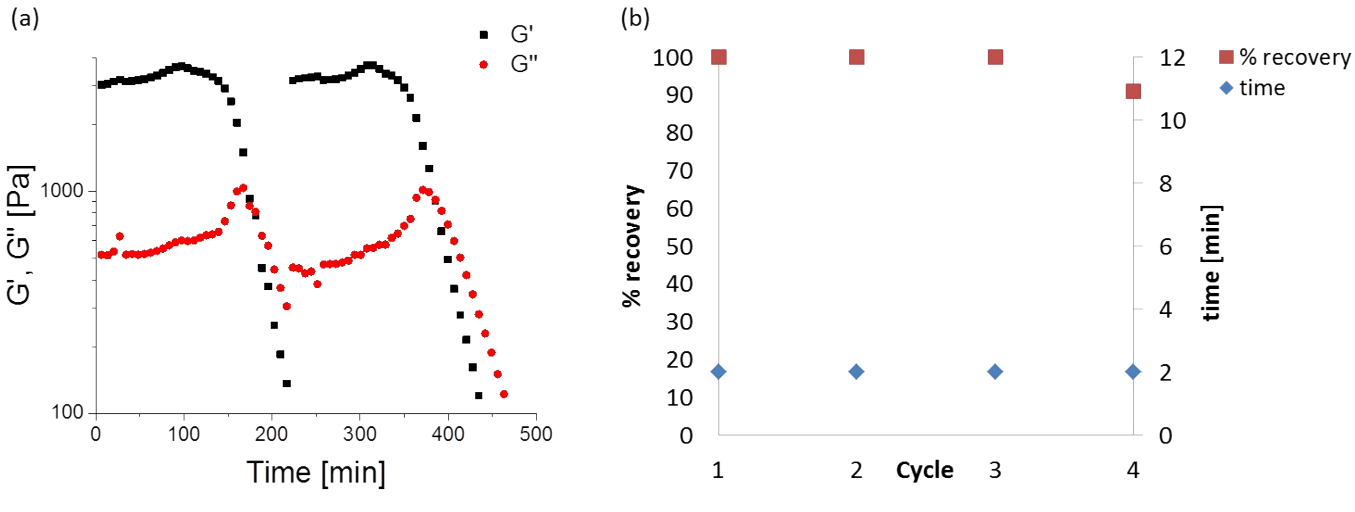

Figure S8. Self-healing characteristics of $G_{6.5\%\_0.08EDA}$ after a secondary crosslinking with 0.7 mg/mL EDA solution. (a) An immediate and full recovery of the networks was achieved. (b) The recovery time required for self-healing of the gel was 2 min and remained constant upon 4 continuous breaking-healing cycles, indicating a significantly faster recovery time than $G_{6.5\%\_0.08EDA}$ (>12 min). Faster recovery time is attributed to a higher content of dynamic imine bonds.

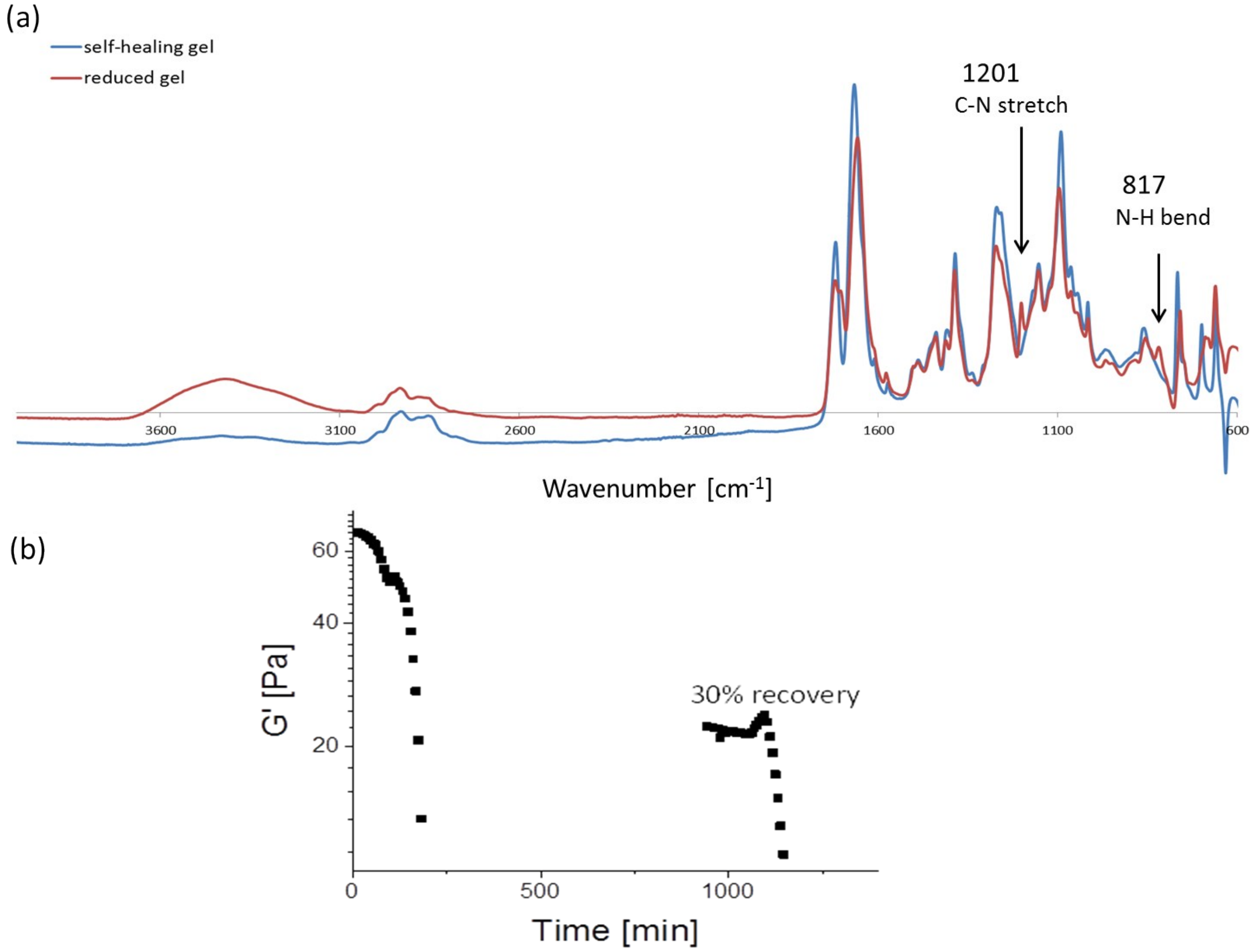

Figure S9. Control experiment: $G_{6.5\%\_0.08EDA}$ was reduced with sodium borohydride to convert dynamic imine bonds to amines. (a) FTIR spectrum of $G_{6.5\%\_0.08EDA}$ (self-healing gel) and $G_{6.5\%\_0.08EDA}$ after reduction (reduced gel): After the reduction, the spectrum reveals a formation of new absorbance bands, attributed to amine bonds: 1201 cm^{-1} (C-N stretch) and 817 cm^{-1} (N-H bend). (b) Strain sweep experiment of the reduced gel: After the gel was destroyed, only ~30% of the networks recovered after 12 min and remained constant with time (in contrast to the self-healing gel, which reaches ~98% recovery). The partial recovery can be attributed to a small fraction of residual imines remaining in the networks, and to a partial stabilization of the networks by hydrogen bonding between the hydroxyl groups present on PHEMA backbone.

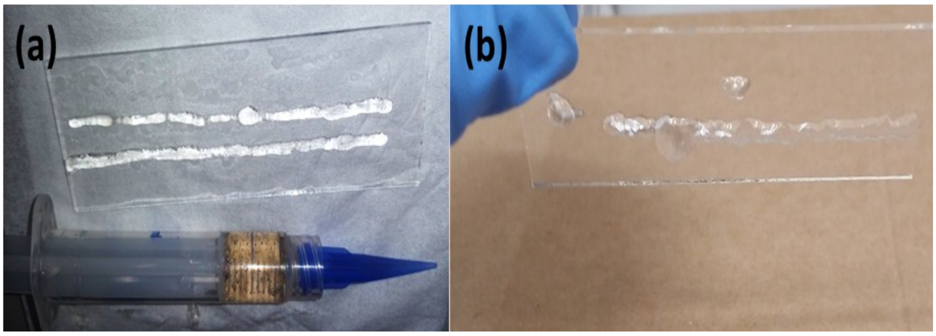

Figure S10. Basic printability assessment of ink formulations. Self-healing gels were loaded into a simple syringe with an attached nozzle (200 and 400 micron diameter), and manually pushed through. Filamentous ink strands, which exited the nozzle, were evaluated for their structural fidelity, typically by a simple inversion of the glass. (a) Soft and extrudable gels with a high printing potential would exhibit a fine filamentous shape, be extruded without a need for applying exceedingly high forces, retain their shape and allow a deposition of a few ink layers on top of each other. (b) Soft and spreadable gels would spread upon the inversion of their substrate due to an exceedingly fluidic nature.

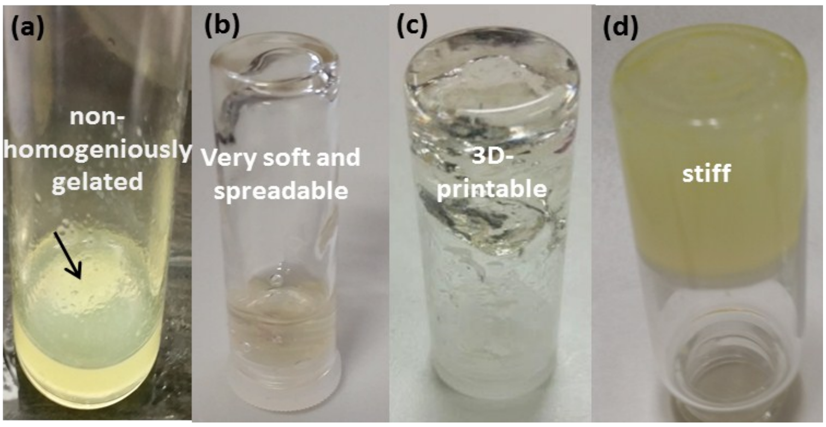

Figure S11. Gels prepared from PHEMA$_{0.35}$-*co*-P4FBA$_{0.65}$ cross-linked with EDA: (a) A non-homogeneous gel is formed when neat EDA is directly introduced to the dissolved polymer. Local “islands” of solid gel (marked by an arrow) are dispersed in the unsolidified liquid. (b) Soft and spreadable gel: this gel is very soft and is an easily flowing solid; however, its spreadable and unstable nature makes it unsuitable for fabrication of 3D-printable, self-supporting structures. (c) 3D-printable gel: a well-balanced gel, which is soft enough to flow and stiff enough to retain its structural integrity. (d) Stiff gel: a non-flowing, stiff and extrusion-resisting gel.

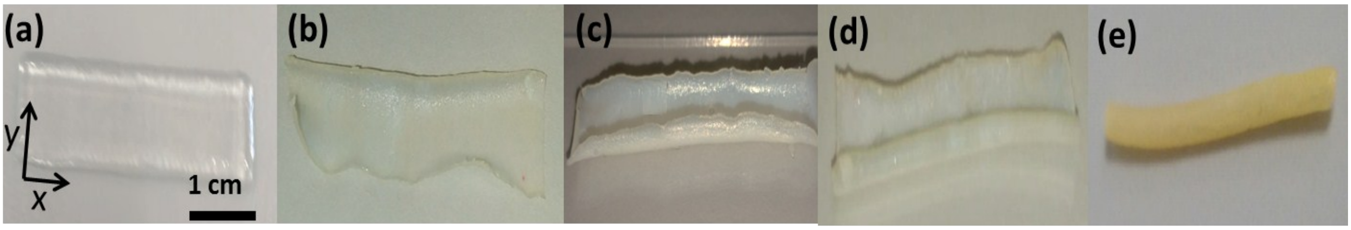

Figure S12. Dry self-assembly of the 3D-printed rectangular object: With the progress of drying, the rectangle re-orients from its planar sheet geometry to a cylinder (“cigar” shape). A gradual rolling over the y axis occurs with drying: (a) A 3D-printed $G_{6.5\%\_0.08EDA}$ rectangle (w=1.0 cm, L=2.5 cm, z=1.0 mm) immediately after printing. (b) After a secondary cross-linking, drying, and detachment from the glass, the 3D-printed rectangle exhibits a locally stress-induced edges wrinkling, as a first step towards rolling. (c-d) Rolling through the y axis. After the initial wrinkling of the edges, the object starts to self-assemble into a more defined, cylindrical shape. (e) A final configuration of the fully rolled, self-assembled cylindrical rod (“cigar”).

References

(1) K. Štulík, K, V. Pacáková, and M. Tichá, *J. Biochem. Biophys. Methods*, 2003, **56**, 1-13.